



Array gain of DIFAR-like sensors

J. N. Maksym

Defence Research Establishment Atlantic

Technical Memorandum

DREA TM 2001-204

December 2001

This page intentionally left blank.

Array gain of DIFAR-like sensors

J. N. Maksym

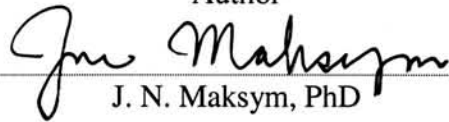
Defence Research Establishment Atlantic

Technical Memorandum

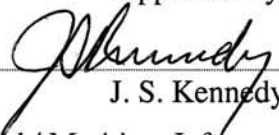
DREA TM 2001-204

December 2001

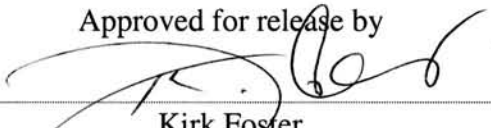
Author


J. N. Maksym, PhD

Approved by


J. S. Kennedy
Head / Maritime Information Systems

Approved for release by


Kirk Foster
Chair / Document Review Panel

© Her Majesty the Queen as represented by the Minister of National Defence, 2001

© Sa majesté la reine, représentée par le ministre de la Défense nationale, 2001

Abstract

This technical memorandum presents a theoretical comparison of array gains obtained with conventional and adaptive beamforming of DIFAR-like sensors. For the purposes of the memorandum, a DIFAR-like sensor is modeled by an omnidirectional element and two orthogonal horizontal dipole elements. Also considered, is an extended DIFAR-like sensor, in which the three-element sensor module is augmented by two horizontal quadrupole elements. A difficult problem in the design of beamformers is how to decide when to use an adaptive beamforming algorithm rather than a conventional beamformer. Basing the decision on data observed during sea trials can be misleading because the relative performance depends heavily on the acoustic environment. The problem can be simplified by comparisons of candidate beamforming techniques with a set of baseline acoustic noise backgrounds, namely 2D and 3D isotropic noise, with the addition of one or two discrete-bearing sources of interference. Mathematical expressions for array gain are derived, and graphical results are shown for the baseline acoustic noise backgrounds. It should be noted that the calculations in this memorandum have assumed that sensor self noise is negligible compared to background noise. This is not likely to be true in practice, especially with dipole and quadrupole sensing elements. To take self noise into account, one needs only to add the appropriate sensor self-noise powers to the diagonal of the cross spectral density matrix in the array gain expressions.

Resume

Ce document technique présente une comparaison théorique des gains de réseau obtenus au moyen de capteurs de type DIFAR à mise en forme adaptative et classique des faisceaux. Aux fins du document, un capteur de type DIFAR est modélisé par un élément omnidirectif et deux éléments bipolaires horizontaux orthogonaux. Le document examine aussi un capteur de type DIFAR élargi, où le module de détection à trois éléments est complété par deux éléments quadripolaires horizontaux. Un problème épineux de conception des conformateurs de faisceaux consiste à décider quand utiliser un algorithme de mise en forme adaptative de faisceaux plutôt qu'un conformateur classique. Le fait de fonder la décision sur les données obtenues durant les essais en mer peut induire en erreur, du fait que la performance relative dépend fortement de l'environnement acoustique. Le problème peut être simplifié par des comparaisons entre les techniques possibles de mise en forme des faisceaux et divers ensembles de bruit de fond acoustique de référence, notamment du bruit isotrope 2D et 3D, avec l'ajout d'une ou de deux sources de brouillage à relèvement discret. Les expressions mathématiques du gain de réseau sont établies, et les résultats graphiques sont montrés pour les ensembles de bruit de fond acoustique de référence. Il est à noter que les calculs du document reposent sur l'hypothèse que le bruit propre des capteurs est négligeable par rapport au bruit de fond. Ce n'est probablement pas vrai en pratique, surtout dans le cas des éléments de détection bipolaires et quadripolaires. Pour tenir compte du bruit propre, il suffit d'ajouter la puissance appropriée du bruit propre des capteurs à la diagonale de la matrice de densité interspectrale dans les expressions du gain de réseau.

Executive summary

Introduction and Background

The acoustic sensor module in a DIFAR sonobuoy is a small acoustic array that is usually modeled as three co-located sensing elements: an omnidirectional hydrophone and two orthogonal horizontal dipoles. For this idealized three-element sensor, the theoretically maximum array gains are 6 dB in a 3D isotropic noise background and 4.77 dB in a 2D isotropic noise background, although in practice lower array gain can result due to system imperfections or self-noise levels that are equal or greater than ambient noise levels. In a non-isotropic noise background, or when there are discrete-bearing interferences, the maximum array gain can be much higher than the abovementioned values. High array gain may sometimes be obtained with a conventional (fixed) beamformer if an interference falls exactly upon a null in the directional response of the beamformer. However, a more consistent way to maximize array gain is to use an adaptive beamformer, such as the MVDR (minimum variance distortionless response) algorithm.

Results

Array gain expressions are developed for the three-element DIFAR-like sensor in a number of ambient noise backgrounds, including 2D and 3D isotropic background noise alone, and also with either one or two discrete-bearing interferences.

Next, a five-element DIFAR-like sensor is considered, in which the three-element sensor is augmented by two horizontal quadrupoles. Array gain expressions are derived for the five-element sensor in the same backgrounds as above. It is shown that, for the five-element sensor, the theoretically maximum array gains are 8.45 dB in a 3D isotropic noise background and 6.99 dB in a 2D isotropic noise background.

Significance

Growing interest in airborne multistatic detection and localization has generated a need to look at more capable sonobuoy sensors. One possibility that has received a good deal of international attention is to configure the sonobuoy sensor as an array of hydrophones. This technical memorandum examines an alternative approach, in which a small array of directional elements is used. It is shown that the addition of two quadrupole elements to a standard DIFAR sensor can considerably increase the array gain in isotropic noise backgrounds, and greatly improve performance in background noise fields dominated by directional sources of interference.

Future Plans

Further work is planned to relate the theoretical results in this technical memorandum to array gains measured with data from experiments at sea. Self noise of the sensor elements is one factor that can reduce the maximum array gains, and needs to be examined further. At present, experimental data from a five-element DIFAR-like acoustic module is not available. However, it is possible to generate both three-element data and five-element data from recordings made with a small ring array containing at least four omnidirectional hydrophones.

An array consisting of two or more DIFAR-like modules is a potentially attractive sensor configuration for multistatic active operation. Such an array can provide array gain improvement over a single DIFAR-like sensor as well as enhanced directional response. A theoretical analysis of the array gains achievable with such configurations is planned. If promising, this may be followed by construction of an experimental array of DIFAR-like sensors, and experimental validation during active sonar trials. Initial experiments would be conducted with a small array of DIFAR sensor modules, with a separate sonobuoy rf channel for each sensor module.

Maksym, Joseph N. 2001. Array gain of DIFAR-like sensors. DREA TM 2001-204. Defence Research Establishment Atlantic.

Sommaire

Introduction et contexte

Le module de détection acoustique d'une bouée acoustique DIFAR est un petit réseau acoustique normalement modélisé par trois éléments de détection co-implantés : un hydrophone omnidirectionnel et deux éléments bipolaires horizontaux orthogonaux. Pour ce capteur à trois éléments idéalisé, les gains maximaux théoriques sont de 6 dB pour un bruit de fond isotrope 3D et de 4,77 dB pour un bruit de fond isotrope 2D, même si, en pratique, on peut noter des gains de réseau plus faibles en raison d'imperfections des systèmes ou de niveaux de bruit propre égaux ou supérieurs aux niveaux du bruit ambiant. Pour un bruit de fond non isotrope ou en présence de sources de brouillage à relèvement discret, le gain de réseau maximal peut être nettement supérieur aux valeurs susmentionnées. Un gain de réseau élevé peut être obtenu à l'occasion au moyen d'un conformateur de faisceaux (fixe) classique lorsque du brouillage arrive exactement dans une zone à rayonnement nul du conformateur. Toutefois, une façon plus uniforme de maximiser le gain de réseau consiste à utiliser un conformateur de faisceaux classique, comme l'algorithme MVDR (réponse sans distorsion à variance minimale).

Résultats

Les expressions du gain de réseau sont établies pour des capteurs de type DIFAR à trois éléments avec un certain nombre d'ensembles de bruit de fond, y compris le bruit de fond isotrope 2D et 3D uniquement, et aussi en présence d'une ou de deux sources de brouillage à relèvement discret.

Le document examine ensuite un capteur de type DIFAR à cinq éléments, où le capteur à trois éléments est complété par deux éléments quadripolaires horizontaux. Les expressions du gain de réseau sont établies pour le capteur à cinq éléments dans

les mêmes conditions de bruit de fond que ci-dessus. Il ressort que, pour le capteur à cinq éléments, les gains de réseau maximaux théoriques sont de 8,45 dB pour un bruit de fond isotrope 3D et de 6,99 dB pour un bruit de fond isotrope 2D.

Importance

Un intérêt croissant à l'égard de la localisation et de la détection multistatique aériennes a suscité le besoin d'examiner des capteurs de bouée acoustique d'un rendement supérieur. Sur la scène internationale, la configuration du capteur de bouée acoustique comme un réseau d'hydrophones a fait naître beaucoup d'intérêt. Le document technique examine une autre approche, où un petit réseau d'éléments directifs est utilisé. Il ressort que l'ajout de deux éléments quadripolaires à un capteur DIFAR standard peut augmenter considérablement le gain de réseau dans les conditions de bruit de fond isotrope et améliorer grandement la performance dans les zones de bruit de fond dominées par des sources directives de brouillage.

Plans pour l'avenir

D'autres travaux sont prévus en vue de l'établissement d'un rapport entre les résultats théoriques présentés dans le document technique et les gains de réseau mesurés lors d'essais en mer. Le bruit propre des éléments de détection est un facteur qui peut réduire le gain de réseau maximal, et il doit faire l'objet d'un examen plus approfondi. À l'heure actuelle, on ne dispose pas de données expérimentales d'un module acoustique de type DIFAR à cinq éléments. Il est cependant possible de générer des données de dispositifs à trois éléments et à cinq éléments à partir d'enregistrements effectués au moyen d'un petit réseau en anneau contenant au moins quatre hydrophones omnidirectifs.

Un réseau composé d'au moins deux modules de type DIFAR constitue une configuration de détection qui pourrait s'avérer intéressante pour l'exploitation active multistatique. Un tel réseau peut offrir un meilleur gain qu'un seul capteur de type

DIFAR et de meilleures caractéristiques de directivité. Une analyse théorique des gains possibles dans de telles configurations est prévue. Si les résultats sont prometteurs, il se peut que l'analyse soit suivie par la construction d'un réseau expérimental de capteurs de type DIFAR, puis par une validation expérimentale durant des essais de sonars actifs. Les premières expériences seraient menées au moyen d'un petit réseau de modules de détection DIFAR, un canal RF distinct de bouée acoustique étant prévu pour chaque module de détection.

Maksym, Joseph N. 2001. Array gain of DIFAR-like sensors (gain de réseau des capteurs de type DIFAR). Document technique 2001-204 du CRDA. Centre de recherches pour la défense Atlantique.

Table of contents

Abstract.....	i
Resume	ii
Executive summary	iii
Introduction and Background.....	iii
Results	iii
Significance	iii
Future Plans.....	iv
Sommaire.....	v
Introduction et contexte.....	v
Résultats	v
Importance	vi
Plans pour l’avenir.....	vi
Table of contents	ix
List of figures	xi
1. Introduction	1
2. Array gain definitions.....	3
2.1 Array gain for a multi-element linear array.....	3
2.2 Alternative expression for distortionless response case	5
2.3 Array gain for time delay and sum beamformer.....	5
2.4 MVDR array gain when Φ_{nn} is known	5
2.5 MVDR array gain when Φ_{nn} is unknown	6
2.6 Array gain for a normalized MVDR beamformer	6
3. Cross-spectral density for sensor elements in isotropic noise	8
3.1 Cross-spectral density between omnidirectional hydrophones.....	8
3.2 Cross-spectral density for sensor elements in 3D isotropic noise	9
3.3 Cross-spectral density for sensor elements in 2D isotropic noise	10

4. Array Gain for a DIFAR sensor module.....	12
4.1 3D isotropic noise.....	12
4.2 2D isotropic noise.....	12
5. Array Gain for an extended DIFAR sensor module	14
5.1 3D isotropic noise.....	14
5.2 2D isotropic noise.....	14
6. Array gain in a non-isotropic background.....	16
6.1 Background consisting of isotropic noise and discrete far-field interferences	16
6.2 DIFAR sensor in 3D isotropic noise and one discrete interference.....	17
6.3 Extended DIFAR sensor in 3D isotropic noise and one discrete interference.....	20
6.4 DIFAR sensor in 2D isotropic noise and one discrete interference.....	22
6.5 Extended DIFAR sensor in 2D isotropic noise and one discrete interference.....	25
6.6 Background consisting of isotropic noise and two discrete interferences	27
6.7 DIFAR sensor in 3D isotropic noise and two discrete interferences.....	27
6.8 DIFAR sensor in 2D isotropic noise and two discrete interferences.....	29
6.9 Extended DIFAR sensor in 3D isotropic noise and two discrete interferences....	31
6.10 Extended DIFAR sensor in 2D isotropic noise and two discrete interferences..	32
7. Discussion of results.....	34
8. References	36
Annex A.....	37
A.1 Cross-spectral density matrix for an extended DIFAR sensor module in 3D isotropic noise.....	37
A.1.1 Cross-spectral terms for an extended DIFAR module	37
Annex B.....	39
B.1 Cross-spectral density matrix for an extended DIFAR sensor module in 2D isotropic noise.....	39
B.1.1 Cross-spectral terms for an extended DIFAR module.....	39

List of figures

Figure 1. Coordinate systems for calculating cross spectral density.	9
Figure 2. Directional response of sensor elements	10
Figure 3. Array gain of an optimized limaçon beam in 3D isotropic noise with a discrete interference at bearing β and power ratio μ	18
Figure 4. Array gain for an MVDR beam in 3D isotropic noise with a discrete interference at bearing β and power ratio μ	19
Figure 5. Relative Array Gain (RAG) for an MVDR beam in 3D isotropic noise with a discrete interference at bearing β and power ratio μ	19
Figure 6. Array gain of an optimized conventional beam in 3D isotropic noise with a discrete interference at bearing β and power ratio μ	20
Figure 7. Array gain for an MVDR beam in 3D isotropic noise with a discrete interference at bearing β and power ratio μ	21
Figure 8. Relative Array Gain (RAG) for an MVDR beam in 3D isotropic noise with a discrete interference at bearing β and power ratio μ	22
Figure 9. Array gain of an optimized limaçon beam in 2D isotropic noise with a discrete interference at bearing β and power ratio μ	23
Figure 10. Array gain for an MVDR beam in 2D isotropic noise with a discrete interference at bearing β and power ratio μ	24
Figure 11. Relative Array Gain (RAG) for an MVDR beam in 2D isotropic noise with a discrete interference at bearing β and power ratio μ	24
Figure 12. Array gain of an optimized conventional beam in 2D isotropic noise with a discrete interference at bearing β and power ratio μ	25
Figure 13. Array gain for an MVDR beam in 2D isotropic noise with a discrete interference at bearing β and power ratio μ	26
Figure 14. Relative Array Gain (RAG) for an MVDR beam in 2D isotropic noise with a discrete interference at bearing β and power ratio μ	27

Figure 15. Array gain of an optimized limaçon beam in 3D isotropic noise with discrete interferences at bearings β and γ , and interference-to-isotropic power ratios $\mu_1 = \mu_2 = 2$	28
Figure 16. Array gain for an MVDR beam in 3D isotropic noise with discrete interferences at bearings β and γ , and interference-to-isotropic power ratios $\mu_1 = \mu_2 = 2$	28
Figure 17. Relative array gain for an MVDR beam in 3D isotropic noise with discrete interferences at bearings β and γ , and interference-to-isotropic power ratios $\mu_1 = \mu_2 = 2$	29
Figure 18. Array gain of an optimized limaçon beam in 2D isotropic noise with discrete interferences at bearings β and γ , and interference-to-isotropic power ratios $\mu_1 = \mu_2 = 2$	29
Figure 19. Array gain for an MVDR beam in 2D isotropic noise with discrete interferences at bearings β and γ , and interference-to-isotropic power ratios $\mu_1 = \mu_2 = 2$	30
Figure 20. Relative array gain for an MVDR beam in 2D isotropic noise with discrete interferences at bearings β and γ , and interference-to-isotropic power ratios $\mu_1 = \mu_2 = 2$	30
Figure 21. Array gain of an optimized conventional beam in 3D isotropic noise with discrete interferences at bearings β and γ , and interference-to-isotropic power ratios $\mu_1 = \mu_2 = 2$	31
Figure 22. Array gain for an MVDR beam in 3D isotropic noise with discrete interferences at bearings β and γ , and interference-to-isotropic power ratios $\mu_1 = \mu_2 = 2$	31
Figure 23. Relative array gain for an MVDR beam in 3D isotropic noise with discrete interferences at bearings β and γ , and interference-to-isotropic power ratios $\mu_1 = \mu_2 = 2$	32
Figure 24. Array gain of an optimized conventional beam in 2D isotropic noise with discrete interferences at bearings β and γ , and interference-to-isotropic power ratios $\mu_1 = \mu_2 = 2$	32
Figure 25. Array gain for an MVDR beam in 2D isotropic noise with discrete interferences at bearings β and γ , and interference-to-isotropic power ratios $\mu_1 = \mu_2 = 2$	33
Figure 26. Relative array gain for an MVDR beam in 2D isotropic noise with discrete interferences at bearings β and γ , and interference-to-isotropic power ratios $\mu_1 = \mu_2 = 2$	33

1. Introduction

The acoustic sensor module in a DIFAR sonobuoy is a small acoustic array that is usually modeled as three co-located sensing elements: an omnidirectional hydrophone and two orthogonal horizontal dipoles. It can be readily shown that the theoretically maximum array gain of the three-element sensor is 6 dB in a 3D isotropic noise background and 4.77 dB in a 2D isotropic noise background. One way to increase these array gains is to add two quadrupole elements to the three-element sensor. This is referred to in this memorandum as the five-element sensor. For the five-element sensor, the theoretically maximum array gain is 8.45 dB in a 3D isotropic noise background and 6.99 dB in a 2D isotropic noise background. In practice, the array gain will be less due to sensor self noise and other system imperfections.

In non-isotropic noise backgrounds, or when there is discrete-bearing interference, the array gain can be much higher. High array gain may also be obtained with a conventional (fixed) beamformer if an interference falls exactly upon a null in the directional response of the beamformer. However, a more consistent way to maximize array gain, regardless of the bearing angle of interference sources, is to use an adaptive beamformer such as the MVDR (minimum variance distortionless response) algorithm.

A difficult problem in sonar receiver design is to decide whether adaptive beamforming can provide sufficient improvement in performance over conventional beamforming to justify the additional complexity. Results from adaptive beamforming during sea trials can be misleading because performance is highly dependent on the acoustic background. For this reason it is useful to evaluate the array gain produced by both conventional and adaptive beamformers under a set of standardized acoustic backgrounds, specifically those with 2D and 3D isotropic ambient noise and zero, one, or more discrete-bearing interferences added at various power levels.

In Section 2, the concept of array gain as a measure of beamformer performance is introduced. Some general definitions for array gain in terms of beamformer-weight vector and the cross-spectral matrix are given. The array gain of various beamformers is defined as a function of the cross-spectral density matrix.

In Section 3, the calculation of the cross-spectral density matrix from the directional response functions of the sensor elements is described for 3D and 2D isotropic noise backgrounds. Calculated values for the matrix elements are given in Annex A for 3D isotropic noise, and in Annex B for 2D isotropic noise.

In Section 4, the array gains of the three-element DIFAR-like sensor are derived in 3D and 2D isotropic noise backgrounds.

In Section 5, the array gains of the five-element DIFAR-like sensor are derived in 3D and 2D isotropic noise backgrounds.

In Section 6, a general expression is derived for the array gain in a noise background that includes isotropic ambient noise and discrete-bearing interferences. The general expression is used to obtain specific expressions for the array gains of three-element and five-element sensors in 3D and 2D isotropic noise for cases with one and two discrete-bearing interferences.

Finally, Section 7 concludes with a brief discussion of the results.

A number of illustrative examples presented in this memorandum were produced with MATLAB™ m-files generated by the author.

2. Array gain definitions

2.1 Array gain for a multi-element linear array

An important measure of array-beamformer performance, which appears in the sonar equation is array gain. The array gain G is usually defined as the ratio of signal-to-noise power at the beamformer output to that at the input, i.e., at the individual hydrophone [1,2].

$$G = snr_{out} / snr_{in} . \quad (1)$$

Expressions for array gain of conventional and adaptive arrays can be found in the literature, including several textbooks. Following the development in Dudgeon and Mersereau [3], the frequency-domain beamformer output of an N -element array for a signal component at frequency ω can be defined as

$$y(\omega) = \frac{1}{N} \sum_{i=1}^N W_i(\omega) R_i(\omega) \exp(-j\omega\tau_i), \quad (2)$$

where $R_i(\omega)$ is the Fourier transform of the i^{th} sensor signal, $W_i(\omega)$ is the beamforming weight, and τ_i is the beam-steering delay. The beamformer output in Equation 2 can be written in vector-matrix form as

$$y = \mathbf{w}^\dagger \mathbf{x}, \quad (3)$$

where \dagger denotes complex conjugate transpose, the vector \mathbf{w} is given by

$$\mathbf{w}(\omega) = \frac{1}{N} [W_1(\omega) \exp(j\omega\tau_1), \dots, W_N(\omega) \exp(j\omega\tau_N)]^T, \quad (4)$$

and the signal vector \mathbf{x} is

$$\mathbf{x}(\omega) = [R_1(\omega), \dots, R_N(\omega)]^T. \quad (5)$$

For convenience, explicit mention of the frequency variable ω has been omitted. The expected output power of the beamformer can be expressed as a Hermitian form

$$P = \mathbf{w}^\dagger E\{\mathbf{x}\mathbf{x}^\dagger\} \mathbf{w} = \mathbf{w}^\dagger \mathbf{\Phi} \mathbf{w}, \quad (6)$$

where $E\{ \}$ denotes an ensemble average and $\mathbf{\Phi}$ is the cross-spectral density matrix defined below

$$\Phi(d, \lambda) = \begin{bmatrix} Q_{1,1}(d, \lambda) & \cdot & \cdot & \cdot & Q_{1,n}(d, \lambda) \\ \cdot & \cdot & \cdot & \cdot & \cdot \\ \cdot & \cdot & \cdot & \cdot & \cdot \\ \cdot & \cdot & \cdot & \cdot & \cdot \\ Q_{n,1}(d, \lambda) & \cdot & \cdot & \cdot & Q_{n,n}(d, \lambda) \end{bmatrix}, \quad (7)$$

where the frequency parameter ω is expressed as $2\pi d / \lambda$, where d is the inter-element spacing of the linear array and λ is the wavelength. Since the elements of the sensors in this technical memorandum are assumed to be located at a single point in space, the cross-spectra above are evaluated at $d = 0$. The cross-spectral terms in Equation 7 are evaluated for 3D and 2D isotropic noise in Appendices A and B, respectively.

An expression for array gain can be derived by writing the cross-spectral matrix as the sum of signal and noise terms as follows [2, 3]

$$\Phi = \sigma_s^2 \mathbf{s} \mathbf{s}^\dagger + \sigma_n^2 \Phi_{nn}, \quad (8)$$

where the signal vector, $\mathbf{s} = [s_1(\omega), \dots, s_N(\omega)]^n$, represents an idealized unit signal wave incident on the array sensors. The signal vector is normalized to make $\mathbf{s}^\dagger \mathbf{s} = N$. The noise cross-spectral density matrix Φ_{nn} is normalized so that its trace is equal to N . The quantities σ_s^2 and σ_n^2 denote the average signal power and the average noise power at a single omnidirectional sensor. Consequently the denominator of Equation 1 is given by

$$snr_{in} = \sigma_s^2 / \sigma_n^2. \quad (9)$$

Application of a beamformer, denoted by the vector \mathbf{w} , produces the following total beam-output power

$$P = \sigma_s^2 |\mathbf{w}^\dagger \mathbf{s}|^2 + \sigma_n^2 \mathbf{w}^\dagger \Phi_{nn} \mathbf{w} \quad (10)$$

The numerator of Equation 1 is the ratio of the terms in Equation 10. Thus

$$snr_{out} = \frac{\sigma_s^2 |\mathbf{w}^\dagger \mathbf{s}|^2}{\sigma_n^2 \mathbf{w}^\dagger \Phi_{nn} \mathbf{w}}. \quad (11)$$

Substitution from Equations 11 and 9 into Equation 1 gives the array gain

$$G = \frac{|\mathbf{w}^\dagger \mathbf{s}|^2}{\mathbf{w}^\dagger \Phi_{nn} \mathbf{w}} = \frac{\mathbf{w}^\dagger \mathbf{s} \mathbf{s}^\dagger \mathbf{w}}{\mathbf{w}^\dagger \Phi_{nn} \mathbf{w}}. \quad (12)$$

2.2 Alternative expression for distortionless response case

An alternative expression for array gain restricted to beamforming vectors for which $\mathbf{w}^\dagger \mathbf{s} = 1$ is given by Van Veen [4]. It describes the array gain as a filtering operation achieved by \mathbf{w} relative to that at a single sensor. To obtain this alternative expression for array gain, assume that \mathbf{w} is derived from an unnormalized matrix $\Phi_{uu} = \sigma_n^2 \Phi_{mm}$, but is subject to the constraint that $\mathbf{w}^\dagger \mathbf{s} = 1$. The beam-output noise power is then given by $\mathbf{w}^\dagger \Phi_{uu} \mathbf{w}$ and the single-hydrophone noise power is given by $[\Phi_{uu}]_{1,1}$. Substitution into Equation 1 gives the array gain expression

$$G = \frac{\sigma_s^2}{\mathbf{w}^\dagger \Phi_{uu} \mathbf{w}} \bigg/ \frac{\sigma_s^2}{[\Phi_{uu}]_{1,1}} = \frac{[\Phi_{uu}]_{1,1}}{\mathbf{w}^\dagger \Phi_{uu} \mathbf{w}}. \quad (13)$$

It should be noted that the first hydrophone noise power is taken as typical of the whole array. This assumes equal noise power in each array sensor.

2.3 Array gain for time delay and sum beamformer

Equation 12 is a general expression for array gain. It is useful to examine specific expressions for G for various beamformers. First, let us consider the simple time delay and sum beamformer. For a beam defined by the signal-direction vector \mathbf{s} , the time delay and sum beamformer is the vector $\mathbf{w}_1 = \mathbf{s} / N$. Upon substitution into Equation 12, the array gain, labeled G_1 , is given by

$$G_1 = \frac{\mathbf{s}^\dagger \mathbf{s}}{\mathbf{s}^\dagger \Phi_{mm} \mathbf{s}} = \frac{N^2}{\mathbf{s}^\dagger \Phi_{mm} \mathbf{s}}. \quad (14)$$

If the noise is uncorrelated between sensors ($\Phi_{mm} = \mathbf{I}$), and G_1 is equal to N .

2.4 MVDR array gain when Φ_{mm} is known

When the noise-only cross-spectral matrix is known, or can be estimated from the data, it is possible to obtain a beamformer-coefficient vector that minimizes the beam-output noise variance while maintaining unit response in the desired signal direction. Detection of active sonar echoes and the detection of impulse-like transients fall into this class of problems because the background noise matrix can be accurately measured without significant contributions from the signal itself. The resulting MVDR beamforming vector is given by

$$\mathbf{w}_2 = \frac{\Phi_m^{-1} \mathbf{s}}{\mathbf{s}^\dagger \Phi_m^{-1} \mathbf{s}}. \quad (15)$$

Substitution into Equation 12 gives the array gain expression

$$G_2 = \mathbf{s}^\dagger \Phi_m^{-1} \mathbf{s}. \quad (16)$$

Beam-output power is given by

$$P_2 = \sigma_s^2 + \sigma_n^2 \frac{1}{\mathbf{s}^\dagger \Phi_m^{-1} \mathbf{s}}. \quad (17)$$

2.5 MVDR array gain when Φ_{nn} is unknown

More commonly, the signal is present at the same time, space, and frequency coordinates as the noise and it is not possible to exclude the signal from estimates of the cross-spectral density. In this case, Φ rather than Φ_m is the cross-spectral density matrix. Application of the MVDR technique gives the high-resolution beamformer introduced by Capon [6]. The resulting array gain expression for the Capon beamformer is

$$G_3 = \frac{(\mathbf{s}^\dagger \Phi^{-1} \mathbf{s})^2}{\mathbf{s}^\dagger \Phi^{-1} \Phi_{nn} \Phi^{-1} \mathbf{s}}, \quad (18)$$

with beam power output

$$P_3 = \mathbf{w}_3^\dagger \Phi \mathbf{w}_3 = \frac{1}{\mathbf{s}^\dagger \Phi^{-1} \mathbf{s}}. \quad (19)$$

2.6 Array gain for a normalized MVDR beamformer

In the minimum-variance normalized response (MVNR) beamformer it is desired to normalize the noise power output across beams by dividing the beam power output due to signal and noise by a time averaged estimate of the beam noise power. The desired result is a unit average noise power across all beams. Consider the case where Φ_m is known, and let the unnormalized value be

$$\Phi_{uu} = \sigma_n^2 \Phi_m. \quad (20)$$

The MVNR beamforming vector can be computed as

$$\mathbf{w}_{mvnr} = \frac{\Phi_{uu}^{-1} \mathbf{s}}{\sqrt{\mathbf{s}^\dagger \Phi_{uu}^{-1} \mathbf{s}}} = \frac{\Phi_{nn}^{-1} \mathbf{s}}{\sigma_n \sqrt{\mathbf{s}^\dagger \Phi_{nn}^{-1} \mathbf{s}}}. \quad (21)$$

With this beamforming vector the beam-output power due to noise is given by

$$P_n = \mathbf{w}_{mvnr}^\dagger \Phi_{uu} \mathbf{w}_{mvnr} = 1. \quad (22)$$

When a signal is present the total output power is given by

$$P = \sigma_s^2 \left| \mathbf{w}_{mvnr}^\dagger \mathbf{s} \right|^2 + P_n. \quad (23)$$

Substitution of the MVNR weight vector of Equation 21 into Equation 12 gives the array gain expression

$$G = \frac{snr_{out}}{snr_{in}} = \frac{\sigma_s^2 \left| \mathbf{w}_{mvnr}^\dagger \mathbf{s} \right|^2}{1} \bigg/ \frac{\sigma_s^2}{\sigma_n^2} = \mathbf{s}^\dagger \Phi_{nn}^{-1} \mathbf{s}. \quad (24)$$

This is the same value as G_2 in Equation 16.

3. Cross-spectral density for sensor elements in isotropic noise

3.1 Cross-spectral density between omnidirectional hydrophones

Calculations for the cross-spectral density for the DIFAR-like sensor elements can be carried out with the technique described by Burdic [6] for omnidirectional hydrophones. Assuming a 3D isotropic noise background with angular intensity K , the cross-spectral density between the omnidirectional hydrophones labeled sensor 1 and sensor 2 in Figure 1 is shown [6] to be

$$Q_{12}(d, \lambda) = K \int_{-\pi}^{\pi} \int_{-\pi/2}^{\pi/2} \exp(j \frac{2\pi d}{\lambda} \sin \psi) \cos \psi d\psi d\gamma, \quad (25)$$

where λ is the wavelength and d is the spacing in meters. The angle variables ψ and γ , defined in Figure 1, are convenient for dealing with a linear array of sensors spaced along the x-axis. The angle ψ is the conical angle measured from the zy-plane and the angle γ is the rotation angle measured within the zy-plane. If the integral in Equation 25 is evaluated, it is found that

$$Q_{12}(d, \lambda) = 4\pi K \frac{\sin(2\pi d / \lambda)}{2\pi d / \lambda}. \quad (26)$$

For co-located sensor elements, d is zero so that Equation 25 can be written

$$Q(0, \lambda) = K \int_{-\pi}^{\pi} \int_{-\pi/2}^{\pi/2} \cos \psi d\psi d\gamma, \quad (27)$$

where the subscripts are dropped since elements are assumed to be at the same location. Note that the expression is independent of frequency. Henceforth, $\mathbf{Q}(m, n)$ will be used to define the cross-spectral density between element- m and element- n of the sensor module.

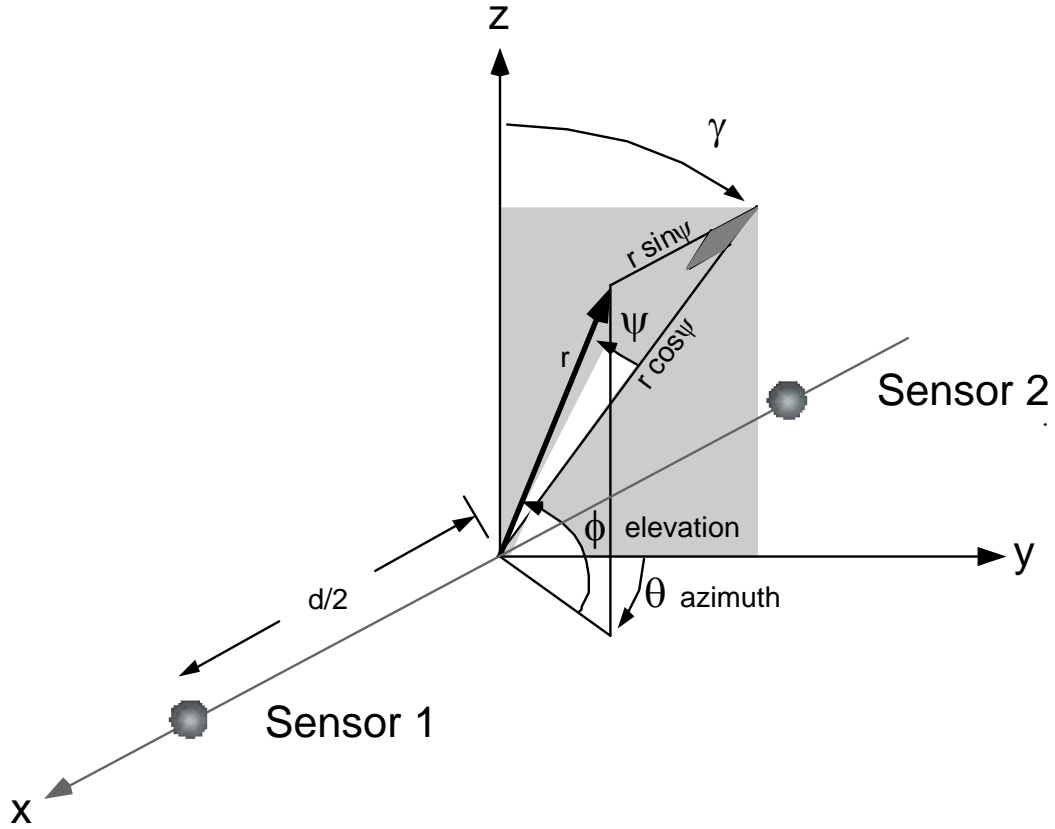


Figure 1. Coordinate systems for calculating cross spectral density.

3.2 Cross-spectral density for sensor elements in 3D isotropic noise

Analogous to Equation 27, the cross-spectral density between element-m and element-n is defined by

$$Q(m, n) = K \int_{-\pi}^{\pi} \int_{-\pi/2}^{\pi/2} D_m(\psi, \gamma) D_n(\psi, \gamma) \cos \psi d\psi d\gamma, \quad (28)$$

where $D_m(\psi, \gamma)$ and $D_n(\psi, \gamma)$ denote the directional response of element-m and element-n respectively.

It is often convenient to work in azimuth-elevation (θ, ϕ) coordinates. Equation 28 in (θ, ϕ) coordinates is

$$Q(m, n) = K \int_{-\pi}^{\pi} \int_{-\pi/2}^{\pi/2} D_m(\theta, \phi) D_n(\theta, \phi) \cos \phi d\phi d\theta. \quad (29)$$

Evaluations of cross-spectra for 3D isotropic noise are given in Annex A.






Element	Response	θ, ϕ Coordinates
0. omnidirectional		1
1. dipole 1		$\cos\theta \cos\phi$
2. dipole 2		$\sin\theta \cos\phi$
3. quadripole 1		$\cos 2\theta \cos\phi$
4. quadripole 2		$\sin 2\theta \cos\phi$

Figure 2. Directional response of sensor elements

3.3 Cross-spectral density for sensor elements in 2D isotropic noise

Evaluation of the cross-spectral densities for an array in 2D isotropic noise is most conveniently accomplished in the θ, ϕ (azimuth-elevation) coordinate system. Following Burdic [6], a 2D isotropic noise model can be obtained from the 3D isotropic one by using a delta function $\delta(\phi - \xi)$ to create a noise model that is isotropic in azimuth, but has an impulse-like distribution $\delta(\phi - \xi)$ in elevation.

The expression for cross-spectral density, equivalent to Equation 29 is given by

$$\begin{aligned}
 Q(m, n) &= K \int_{-\pi}^{\pi} \int_{-\pi/2}^{\pi/2} \delta(\phi - \xi) D_m(\theta, \phi) D_n(\theta, \phi) \cos \phi \, d\phi d\theta \\
 &= K \cos \xi \int_0^{2\pi} D_m(\theta, \xi) D_n(\theta, \xi) \, d\theta.
 \end{aligned}
 \tag{30}$$

Note that when $\xi = 0$, the expression describes the cross-spectrum for a 2D horizontally isotropic noise field with intensity of K units per radian. Evaluations of cross-spectra for 2D horizontally isotropic noise are given in Annex B.

4. Array Gain for a DIFAR sensor module

In this section the array gain for an optimum conventional beamformer for a standard three-element (omnidirectional, x-axis dipole, and y-axis- dipole) DIFAR sensor module is considered. For the three-element sensor, the possible horizontal beam-response patterns are members of the mathematical family of curves called limaçons. The beam-response pattern for the optimized beamformer is one member of this family. Discussion of the results is deferred to Section 7.

4.1 3D isotropic noise

From Equation 29, the cross-spectral matrix for 3D isotropic noise is given by

$$\mathbf{R} = 4\pi K \text{diag}(1, 1/3, 1/3) . \quad (31)$$

Upon normalization by $4\pi K$, the isotropic noise power at the omnidirectional sensor, the cross-spectral matrix can be written as

$$\Phi_{3D} = \text{diag}(1, 1/3, 1/3) . \quad (32)$$

A unit signal vector incident at azimuthal angle θ is given by

$$\mathbf{s}(\theta) = [1, \sin(\theta), \cos(\theta)]^T . \quad (33)$$

Substitution of Equations 32 and 33 into Equation 16 gives the array gain

$$G_{3D} = \mathbf{s}^\dagger \Phi_{3D}^{-1} \mathbf{s} = 4 \quad (6 \text{ dB}) \quad (34)$$

This array gain is achieved by the beamforming vector from Equation 15, given by

$$\mathbf{w}_{3D} = \frac{\Phi_{3D}^{-1} \mathbf{s}}{\mathbf{s}^\dagger \Phi_{3D}^{-1} \mathbf{s}} = 0.25 [1, 3\sin(\theta), 3\cos(\theta)]^T . \quad (35)$$

4.2 2D isotropic noise

From Equation 30, the cross-spectral matrix for 2D isotropic noise is given by

$$\mathbf{R} = 2\pi K \text{diag}(1, 1/2, 1/2) . \quad (36)$$

Upon normalization by $2\pi K$, the isotropic noise power at the omnidirectional sensor, the cross-spectral matrix can be written as

$$\Phi_{2D} = \text{diag}(1, 1/2, 1/2). \quad (37)$$

Substitution of Equations 37 and 33 into Equation 16 gives the array gain

$$G_{2D} = \mathbf{s}^\dagger \Phi_{2D}^{-1} \mathbf{s} = 3 \quad (\cong 4.77 \text{ dB}). \quad (38)$$

This array gain is achieved by the beamforming vector from Equation 15, given by

$$\mathbf{w}_{2D} = \frac{\Phi_{2D}^{-1} \mathbf{s}}{\mathbf{s}^\dagger \Phi_{2D}^{-1} \mathbf{s}} = \frac{1}{3} [1, 2 \sin(\theta), 2 \cos(\theta)]^T. \quad (39)$$

5. Array Gain for an extended DIFAR sensor module

A DIFAR sensor module with omnidirectional, x-axis dipole, y-axis- dipole directional responses is extended by the addition of two orthogonal quadrupole-response elements. In this section the array gain for optimum beamforming of this five-element extended DIFAR sensor module is considered. Discussion of the results is deferred to Section 7.

5.1 3D isotropic noise

From Equation 29, the cross-spectral matrix for 3D isotropic noise is given by

$$\mathbf{R} = 4\pi K \text{diag}(1, 1/3, 1/3, 1/3, 1/3) . \quad (40)$$

Upon normalization by $4\pi K$, the isotropic noise power at the omnidirectional sensor, the cross-spectral matrix can be written as

$$\Phi_{3D} = \text{diag}(1, 1/3, 1/3, 1/3, 1/3) . \quad (41)$$

A unit signal vector incident at azimuthal angle θ is given by

$$\mathbf{s}(\theta) = [1, \sin(\theta), \cos(\theta), \sin(2\theta), \cos(2\theta)]^T . \quad (42)$$

Substitution of Equations 41 and 42 into Equation 16 gives the array gain

$$G_{3D} = \mathbf{s}^\dagger \Phi_m^{-1} \mathbf{s} = 7 \quad (\cong 8.45 \text{ dB}) \quad (43)$$

This array gain is achieved by the beamforming vector from Equation 15, given by

$$\mathbf{w}_{3D} = \frac{\Phi_{3D}^{-1} \mathbf{s}}{\mathbf{s}^\dagger \Phi_{3D}^{-1} \mathbf{s}} = \frac{1}{7} [1, 3 \sin(\theta), 3 \cos(\theta), 3 \sin(2\theta), 3 \cos(2\theta)]^T . \quad (44)$$

5.2 2D isotropic noise

From Equation 30, the cross-spectral matrix for 2D isotropic noise is given by

$$\mathbf{R} = 2\pi K \text{diag}(1, 1/2, 1/2, 1/2, 1/2) . \quad (45)$$

Upon normalization by $2\pi K$, the isotropic noise power at the omnidirectional sensor, the cross-spectral matrix can be written as

$$\Phi_{2D} = \text{diag}(1, 1/2, 1/2, 1/2, 1/2). \quad (46)$$

Substitution of Equations 46 and 42 into Equation 16 gives the array gain

$$G_{2D} = \mathbf{s}^\dagger \Phi_{nm}^{-1} \mathbf{s} = 5 \quad (\cong 6.99 \text{ dB}) \quad (47)$$

This array gain is achieved by the beamforming vector from Equation 15, given by

$$\mathbf{w}_{2D} = \frac{\Phi_{3D}^{-1} \mathbf{s}}{\mathbf{s}^\dagger \Phi_{3D}^{-1} \mathbf{s}} = \frac{1}{5} [1, 2\sin(\theta), 2\cos(\theta), 2\sin(2\theta), 2\cos(2\theta)]^T. \quad (48)$$

6. Array gain in a non-isotropic background

6.1 Background consisting of isotropic noise and discrete far-field interferences

In this Section, a general expression is derived for the array gain in a noise background that includes discrete-bearing interferences. The expression is used to obtain specific expressions for the array gains of three-element and five-element sensors in 3D and 2D isotropic noise for cases with one and two discrete-bearing interferences. Discussion of the results is deferred to Section 7.

In general, for arbitrary arrays, when the noise background contains some number M of discrete far-field interferences, the m^{th} interference adds a term $\sigma_m^2 \mathbf{d}_m \mathbf{d}_m^\dagger$ to the cross-spectral density matrix in Equation 8, where \mathbf{d}_m is an interference-direction vector defined in similar fashion to the signal-direction vector of Equation 8. The resulting total cross-spectral density matrix is then given by

$$\Phi = \sigma_s^2 \mathbf{s} \mathbf{s}^\dagger + \sigma_n^2 \Phi_{nn} + \sum_{m=1}^M \sigma_m^2 \mathbf{d}_m \mathbf{d}_m^\dagger, \quad (49)$$

where σ_m^2 represents the average power of the m^{th} interference as seen by an omnidirectional sensor and Φ_{nn} is the isotropic noise cross-spectral density matrix. The input snr (denominator in Equation 1) is

$$\text{snr}_{in} = \frac{\sigma_s^2}{\sigma_n^2 + \sum_{m=1}^M \sigma_m^2}. \quad (50)$$

Application of a beamforming vector \mathbf{w} produces a total output power given by

$$P = \sigma_s^2 |\mathbf{w}^\dagger \mathbf{s}|^2 + \sigma_n^2 \mathbf{w}^\dagger \Phi_{nn} \mathbf{w} + \sum_{m=1}^M \sigma_m^2 |\mathbf{w}^\dagger \mathbf{d}_m|^2. \quad (51)$$

The output snr (numerator in Equation 1) is given by

$$\text{snr}_{out} = \frac{\sigma_s^2 |\mathbf{w}^\dagger \mathbf{s}|^2}{\sigma_n^2 \mathbf{w}^\dagger \Phi_{nn} \mathbf{w} + \sum_{m=1}^M \sigma_m^2 |\mathbf{w}^\dagger \mathbf{d}_m|^2}. \quad (52)$$

Array gain, from Equation 1, is determined by the ratio

$$G = snr_{out} / snr_{in} = \frac{\left(\sigma_n^2 + \sum_{m=1}^M \sigma_m^2 \right) |\mathbf{w}^\dagger \mathbf{s}|^2}{\sigma_n^2 \mathbf{w}^\dagger \Phi_{nn} \mathbf{w} + \sum_{m=1}^M \sigma_m^2 |\mathbf{w}^\dagger \mathbf{d}_m|^2} \quad (53)$$

For the case of a single discrete interference, define the interference-to-isotropic noise-power ratio as $\mu = \sigma_1^2 / \sigma_n^2$ and let $\mathbf{d} = \mathbf{d}_1$. Then, the array gain expression may be written as

$$G = snr_{out} / snr_{in} = \frac{(1 + \mu) |\mathbf{w}^\dagger \mathbf{s}|^2}{\mathbf{w}^\dagger \Phi_{nn} \mathbf{w} + \mu |\mathbf{w}^\dagger \mathbf{d}|^2}. \quad (54)$$

6.2 DIFAR sensor in 3D isotropic noise and one discrete interference

In the remainder of the section, the array gains for conventional and MVDR beamformers are compared in an isotropic noise background with first one, and then two discrete-bearing sources of interference.

For a three-element sensor the direction vector for a discrete bearing interference at an azimuthal angle β degrees and a power level μ times the isotropic noise power measured at the omnidirectional sensor is given by

$$\mathbf{d}(\beta) = \sqrt{\mu} [1, \sin(\beta), \cos(\beta)]^T. \quad (55)$$

The conventional beamformer used in the comparison is that given by Equation 35 for a steering direction of zero degrees. Substitution of Equation 35 into Equation 54 gives the following expression for the array gain.

$$G(\mu, \beta) = \frac{16(1 + \mu)}{4 + \mu + 6\mu \cos(\beta) + 9\mu \cos^2(\beta)}. \quad (56)$$

In Figure 3, Equation 56 is plotted, for $\mu = 1, 2,$ and $4,$ as a function of the interference bearing β .

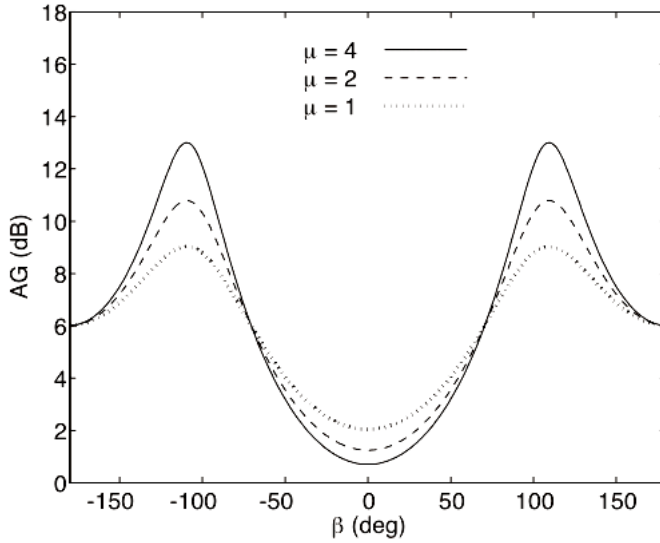


Figure 3. Array gain of an optimized limaçon beam in 3D isotropic noise with a discrete interference at bearing β and power ratio μ .

To calculate the array gain for an MVDR beam steered to zero degrees, the total cross spectral matrix given by Equation 49 is substituted into Equation 15, with the steering vector defined for $\theta = 0$. Note that Equation 49 includes contributions from the signal as well as noise. It is not always possible to form an estimate of the noise part without some contamination by the signal. In the active sonar application, however, the signal is of relatively short duration and contributes only a small amount to the estimate. In the case of negligible signal contribution, the array gain is given by

$$G(\mu, \beta) = \frac{(1 + \mu)(8 + 21\mu - 12\mu \cos(\beta) - 9\mu \cos(2\beta))}{2 + 8\mu}. \quad (57)$$

In Figure 4, Equation 57 is plotted, for $\mu = 1, 2,$ and $4,$ as a function of the interference bearing β .

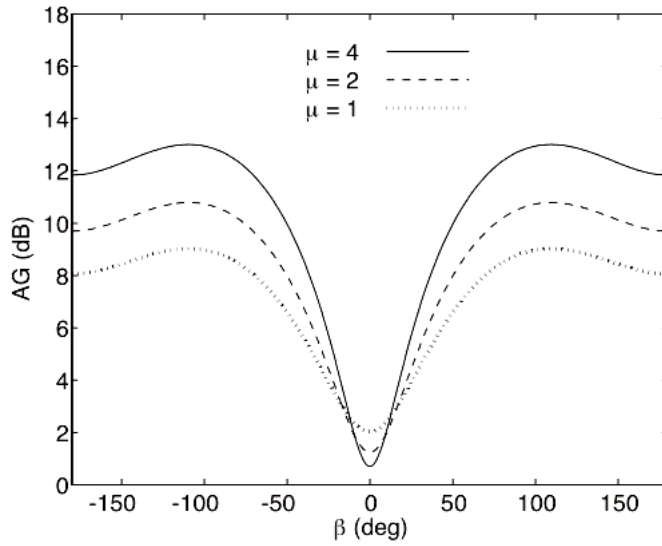


Figure 4. Array gain for an MVDR beam in 3D isotropic noise with a discrete interference at bearing β and power ratio μ .

The increase in array gain obtained with the MVDR beamformer (Figure 4) relative to the conventional one, referred to as the relative array gain (RAG), is plotted in Figure 5.

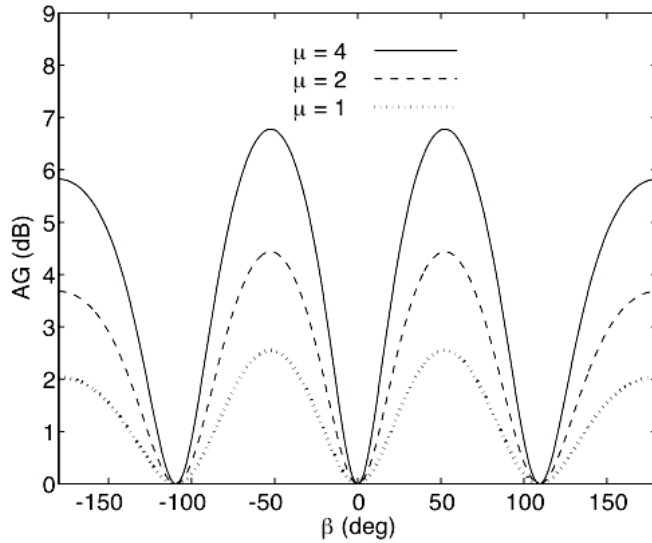


Figure 5. Relative Array Gain (RAG) for an MVDR beam in 3D isotropic noise with a discrete interference at bearing β and power ratio μ .

6.3 Extended DIFAR sensor in 3D isotropic noise and one discrete interference

For the five-element sensor the direction vector for a discrete bearing interference at an azimuthal angle β degrees and a power level μ times the isotropic noise power measured at the omnidirectional sensor is given by

$$\mathbf{d}(\beta) = \sqrt{\mu} [1, \sin(\beta), \cos(\beta), \sin(2\beta), \cos(2\beta)]^T . \quad (58)$$

The conventional beamformer used in the comparison is that given by Equation 44. Substitution of Equation 44 into Equation 54, with $\theta = 0$, gives the following expression for the array gain.

$$G(\mu, \beta) = \frac{49(1+\mu)}{7 + \mu(1 + 3\cos(\beta) + 3\cos(2\beta))^2} . \quad (59)$$

In Figure 6, Equation 59 is plotted, for $\mu = 1, 2$, and 4, as a function of the interference bearing β .

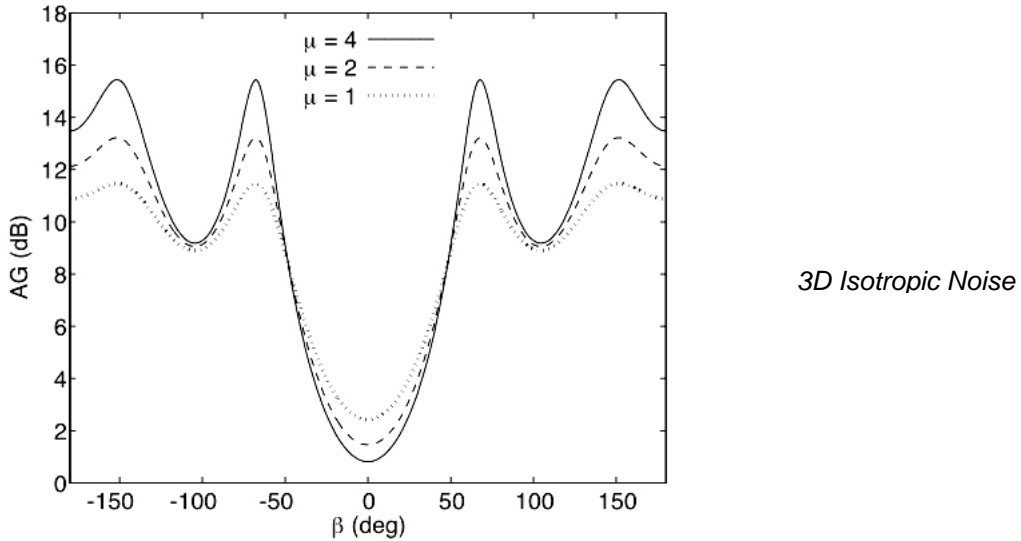


Figure 6. Array gain of an optimized conventional beam in 3D isotropic noise with a discrete interference at bearing β and power ratio μ .

To calculate the array gain for the MVDR beamformer, the total cross spectral matrix given by Equation 49 is substituted into Equation 15 for the steering direction $\theta = 0$, assuming again that the signal contribution can be neglected. Substitution into Equation 54 gives the following expression for the array gain.

$$G(\mu, \beta) = \frac{(1 + \mu)(14 + 78\mu - 30\mu \cos(\beta) - 21\mu \cos(2\beta) - 18\mu \cos(3\beta) - 9\mu \cos(4\beta))}{2 + 14\mu} \dots(60)$$

In Figure 7, Equation 60 is plotted, for $\mu = 1, 2$, and 4 , as a function of the interference bearing β .

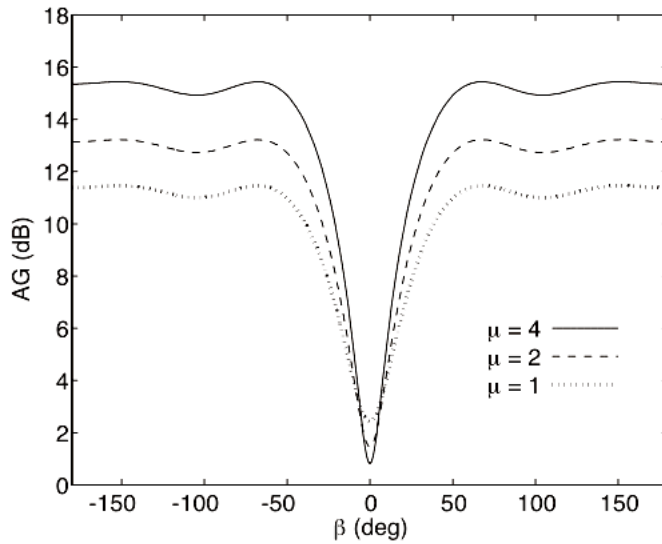


Figure 7. Array gain for an MVDR beam in 3D isotropic noise with a discrete interference at bearing β and power ratio μ .

The relative array gain (RAG) is plotted in Figure 8.

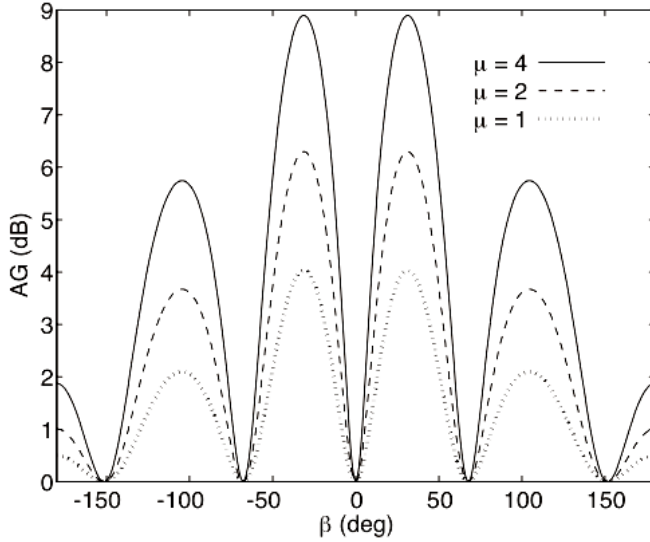


Figure 8. Relative Array Gain (RAG) for an MVDR beam in 3D isotropic noise with a discrete interference at bearing β and power ratio μ .

6.4 DIFAR sensor in 2D isotropic noise and one discrete interference

Assume that the background consists of 2D isotropic noise and the interference direction vector is given by Equation 55. The conventional beamformer used in the comparison is that given by Equation 38. Substitution of Equation 38 into Equation 54, with $\theta = 0$, gives the following expression for the array gain.

$$G(\mu, \beta) = \frac{9(1+\mu)}{3+\mu+4\mu\cos(\beta)+4\mu\cos^2(\beta)}. \quad (61)$$

In Figure 9, Equation 61 is plotted, for $\mu = 1, 2$, and 4 , as a function of the interference bearing β .

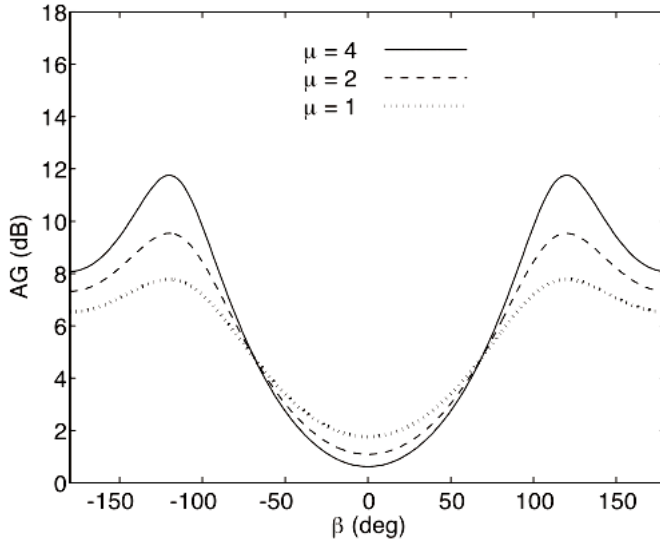


Figure 9. Array gain of an optimized limaçon beam in 2D isotropic noise with a discrete interference at bearing β and power ratio μ .

To calculate the array gain for the MVDR beamformer, the total cross spectral matrix given by Equation 49 is substituted into Equation 15 for the steering direction $\theta = 0$, assuming again that the signal contribution can be neglected. Substitution into Equation 54 gives the following expression for the array gain.

$$G(\mu, \beta) = \frac{(1 + \mu)(3 + 6\mu - 4\mu \cos(\beta) - 2\mu \cos(2\beta))}{1 + 3\mu}. \quad (62)$$

In Figure 10, Equation 62 is plotted, for $\mu = 1, 2,$ and $4,$ as a function of the interference bearing β .

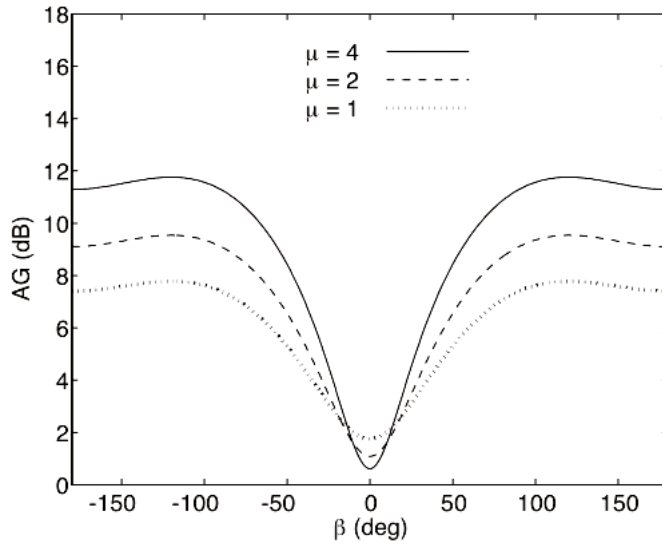


Figure 10. Array gain for an MVDR beam in 2D isotropic noise with a discrete interference at bearing β and power ratio μ .

The relative array gain (RAG) is plotted in Figure 11.

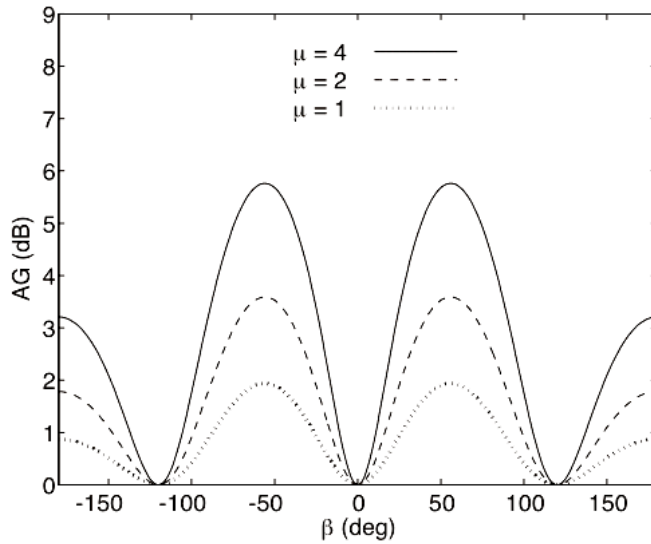


Figure 11. Relative Array Gain (RAG) for an MVDR beam in 2D isotropic noise with a discrete interference at bearing β and power ratio μ .

6.5 Extended DIFAR sensor in 2D isotropic noise and one discrete interference

Assume that the background consists of 2D isotropic noise and the interference direction vector is given by Equation 55. The conventional beamformer used in the comparison is that given by Equation 48. Substitution into Equation 54, with $\theta = 0$, gives the following expression for the array gain.

$$G(\mu, \beta) = \frac{25(1+\mu)}{5+\mu(1+2\cos(\beta)+2\cos(2\beta))^2}. \quad (63)$$

In Figure 12, Equation 63 is plotted, for $\mu = 1, 2$, and 4, as a function of the interference bearing β .

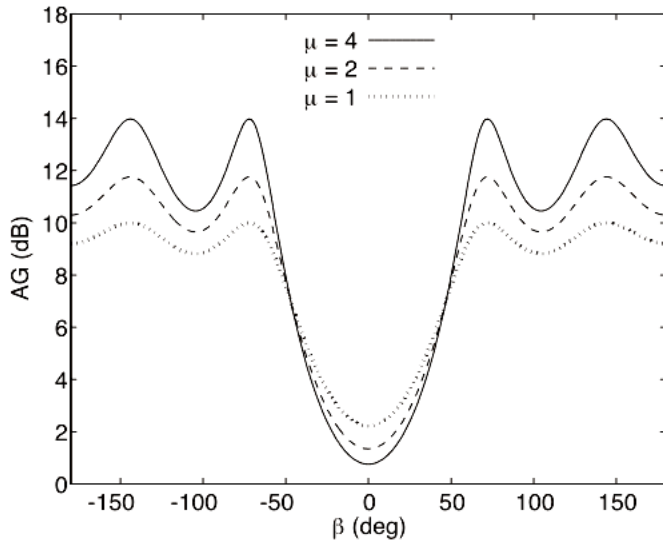


Figure 12. Array gain of an optimized conventional beam in 2D isotropic noise with a discrete interference at bearing β and power ratio μ .

To calculate the array gain for the MVDR beamformer, the total cross spectral matrix given by Equation 49 is substituted into Equation 15 for the steering direction $\theta = 0$, assuming again that the signal contribution can be neglected. Substitution into Equation 54 gives the following expression for the array gain.

$$G(\mu, \beta) = \frac{(1 + \mu)(5 + 20\mu - 8\mu \cos(\beta) - 6\mu \cos(2\beta) - 4\mu \cos(3\beta) - 2\mu \cos(4\beta))}{1 + 5\mu} \dots(64)$$

In Figure 13, Equation 64 is plotted, for $\mu = 1, 2,$ and $4,$ as a function of the interference bearing β .

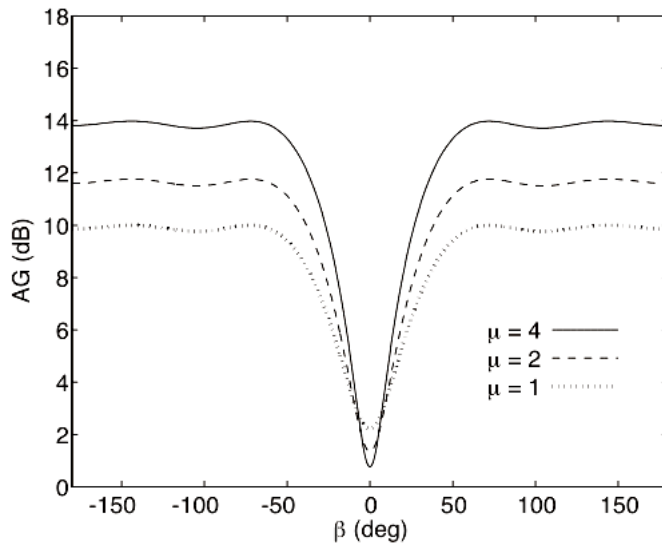


Figure 13. Array gain for an MVDR beam in 2D isotropic noise with a discrete interference at bearing β and power ratio μ .

The relative array gain (RAG) is plotted in Figure 14.

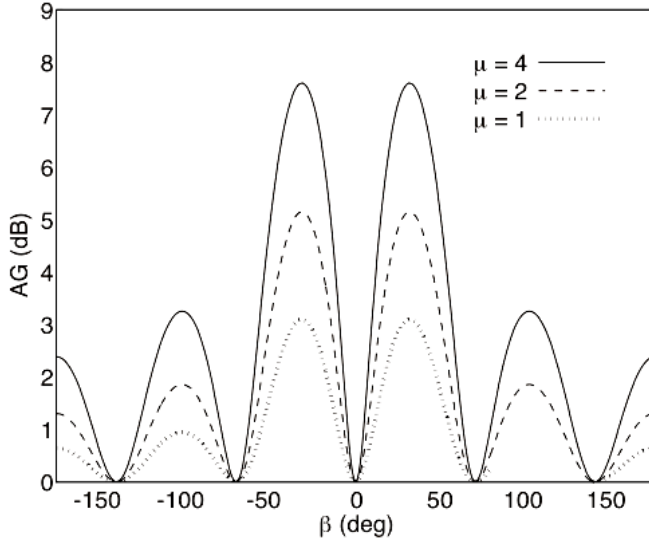


Figure 14. Relative Array Gain (RAG) for an MVDR beam in 2D isotropic noise with a discrete interference at bearing β and power ratio μ .

6.6 Background consisting of isotropic noise and two discrete interferences

For multiple discrete (in bearing) interferences Equation 53 may be expressed as

$$G = snr_{out} / snr_{in} = \frac{\left(1 + \sum_{m=1}^M \mu_m\right) |\mathbf{w}^\dagger \mathbf{s}|^2}{\mathbf{w}^\dagger \Phi_m \mathbf{w} + \sum_{m=1}^M \mu_m |\mathbf{w}^\dagger \mathbf{d}_m|^2}, \quad (65)$$

where, μ_m and \mathbf{d}_m are the interference-to-isotropic power ratio and direction vector of the m^{th} interfering signal wave.

6.7 DIFAR sensor in 3D isotropic noise and two discrete interferences

Figures 15, 16, and 17 show the array gains given by Equation 65 for limaçon beamforming and MVDR beamforming for a three-sensor array, as well as the relative array gain, in backgrounds containing isotropic noise and two discrete interferences.

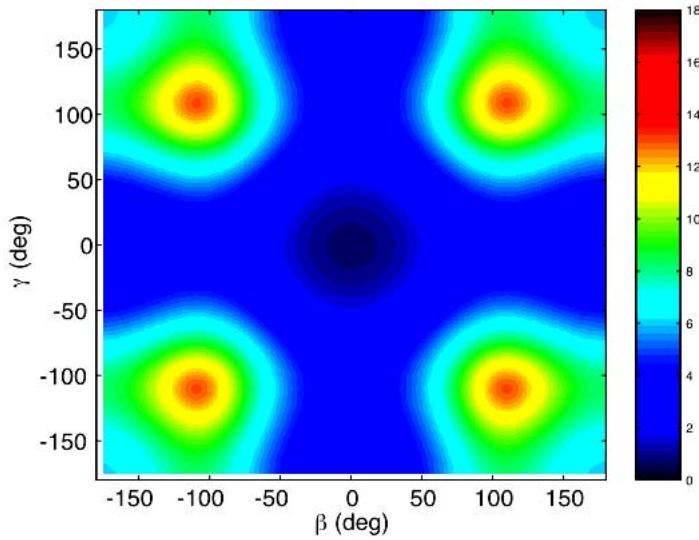


Figure 15. Array gain of an optimized limaçon beam in 3D isotropic noise with discrete interferences at bearings β and γ , and interference-to-isotropic power ratios $\mu_1 = \mu_2 = 2$.

It is informative to compare Figure 15 (two interferences) with Figure 3 (one interference). Values on the diagonals of the plot in Figure 15 correspond to both interferences being at the same bearing angle. The array gains on the diagonal are therefore identical to the values at the same bearing of Figure 3 when $\mu = 4$. Similar comments apply to the other two-interference plots in this section.

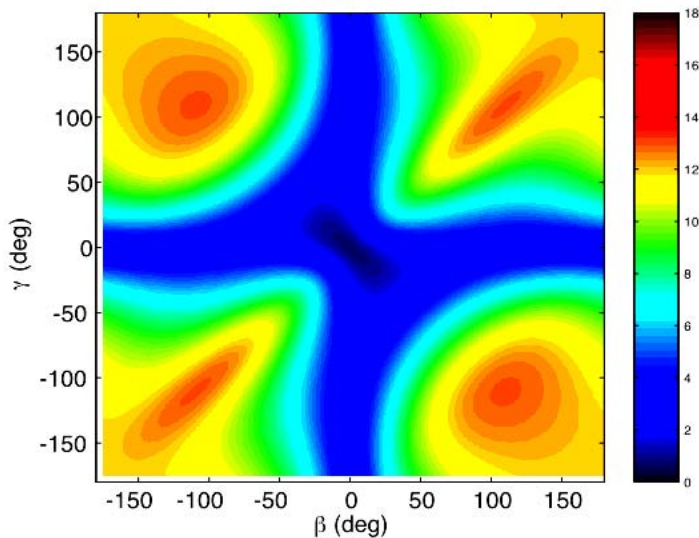


Figure 16. Array gain for an MVDR beam in 3D isotropic noise with discrete interferences at bearings β and γ , and interference-to-isotropic power ratios $\mu_1 = \mu_2 = 2$.

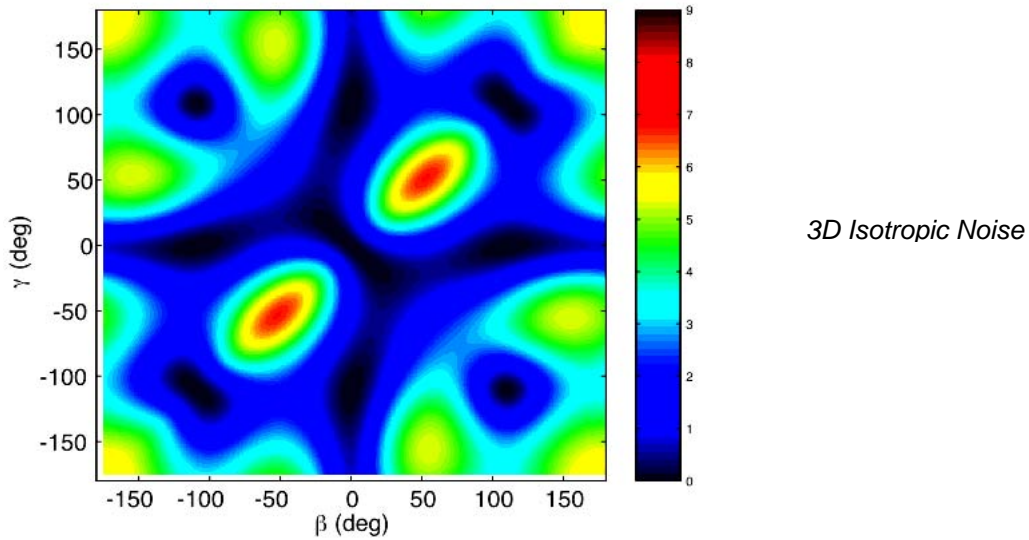


Figure 17. Relative array gain for an MVDR beam in 3D isotropic noise with discrete interferences at bearings β and γ , and interference-to-isotropic power ratios $\mu_1 = \mu_2 = 2$.

6.8 DIFAR sensor in 2D isotropic noise and two discrete interferences

Figures 18, 19, and 20 show the array gains given by Equation 65 for optimized limaçon beamforming, MVDR beamforming, as well as the relative array gain, for backgrounds containing isotropic noise and two discrete interferences.

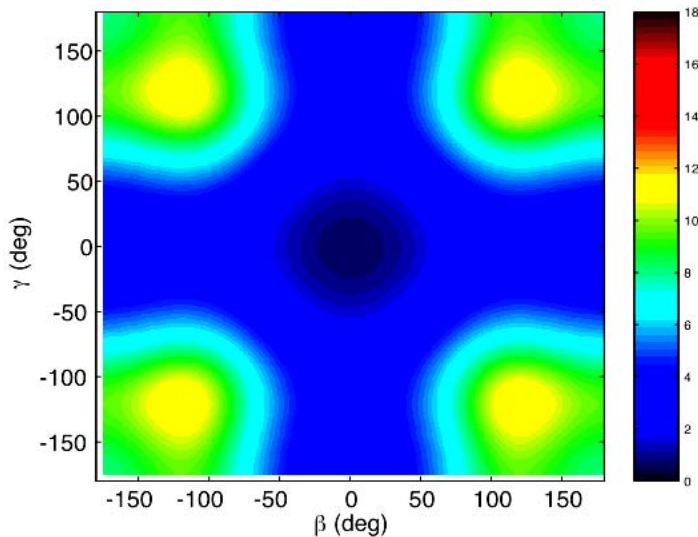


Figure 18. Array gain of an optimized limaçon beam in 2D isotropic noise with discrete interferences at bearings β and γ , and interference-to-isotropic power ratios $\mu_1 = \mu_2 = 2$.

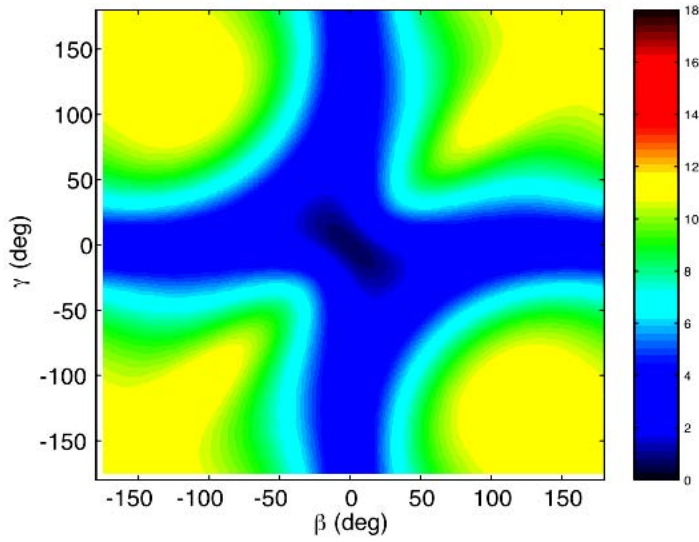


Figure 19. Array gain for an MVDR beam in 2D isotropic noise with discrete interferences at bearings β and γ , and interference-to-isotropic power ratios $\mu_1 = \mu_2 = 2$.

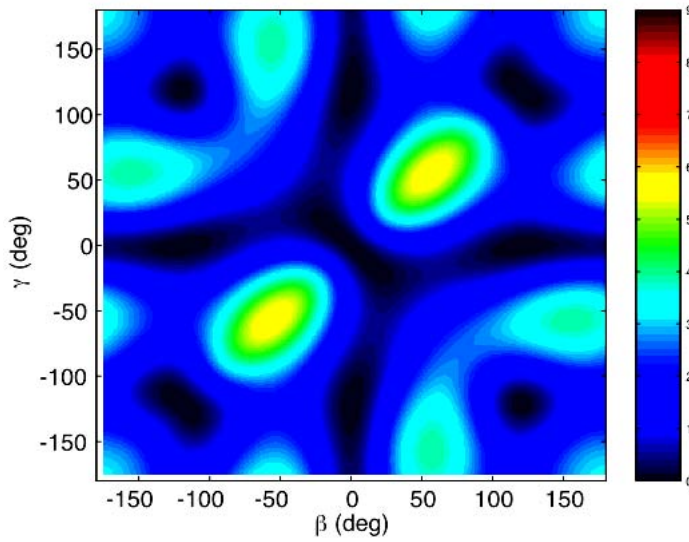


Figure 20. Relative array gain for an MVDR beam in 2D isotropic noise with discrete interferences at bearings β and γ , and interference-to-isotropic power ratios $\mu_1 = \mu_2 = 2$.

6.9 Extended DIFAR sensor in 3D isotropic noise and two discrete interferences

Figures 21, 22, and 23 show the array gains given by Equation 65 for conventional beamforming, MVDR beamforming, as well as the relative array gain, for backgrounds containing isotropic noise and two discrete interferences.

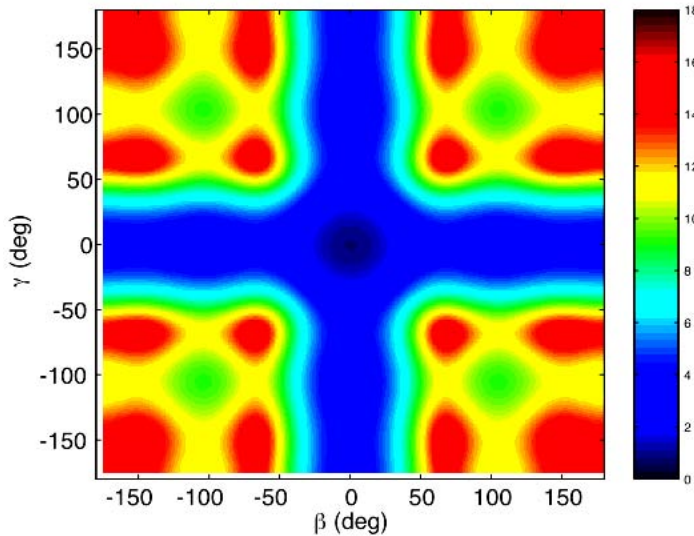


Figure 21. Array gain of an optimized conventional beam in 3D isotropic noise with discrete interferences at bearings β and γ , and interference-to-isotropic power ratios $\mu_1 = \mu_2 = 2$.

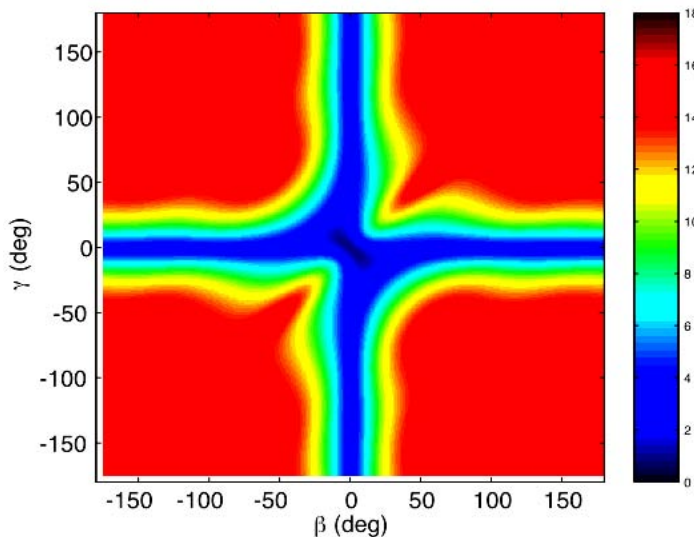


Figure 22. Array gain for an MVDR beam in 3D isotropic noise with discrete interferences at bearings β and γ , and interference-to-isotropic power ratios $\mu_1 = \mu_2 = 2$.

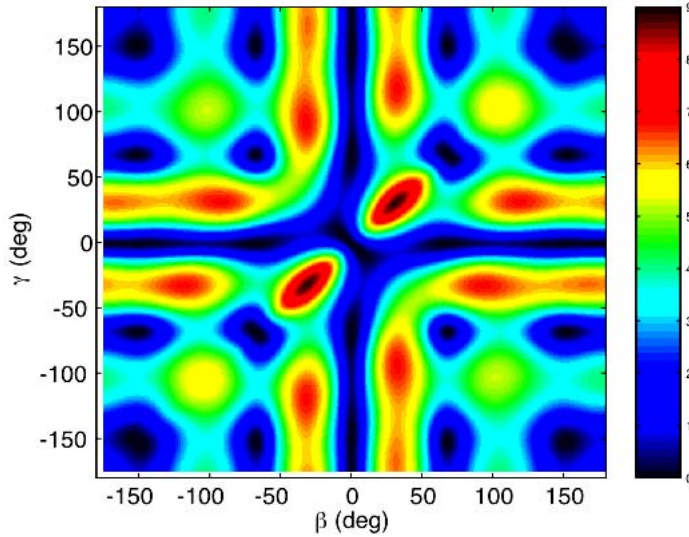


Figure 23. Relative array gain for an MVDR beam in 3D isotropic noise with discrete interferences at bearings β and γ , and interference-to-isotropic power ratios $\mu_1 = \mu_2 = 2$.

6.10 Extended DIFAR sensor in 2D isotropic noise and two discrete interferences

Figures 24, 25, and 26 show the array gains given by Equation 65 for optimized conventional beamforming, MVDR beamforming, and the relative array gain, respectively, for backgrounds containing isotropic noise and two discrete interferences.

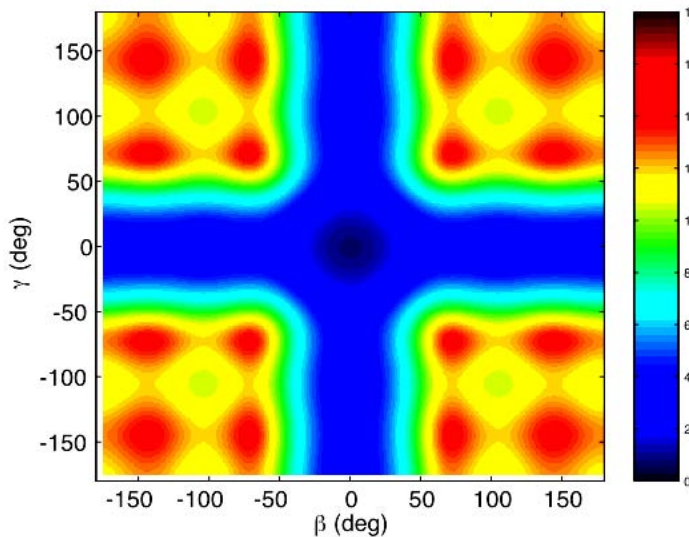


Figure 24. Array gain of an optimized conventional beam in 2D isotropic noise with discrete interferences at bearings β and γ , and interference-to-isotropic power ratios $\mu_1 = \mu_2 = 2$.

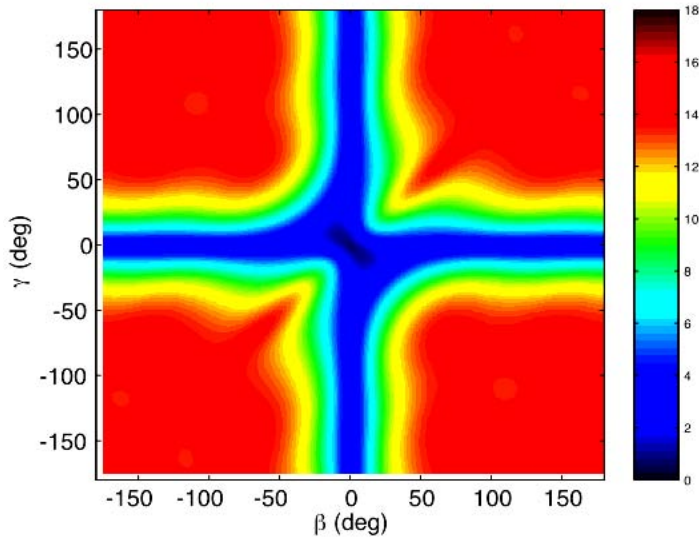


Figure 25. Array gain for an MVDR beam in 2D isotropic noise with discrete interferences at bearings β and γ , and interference-to-isotropic power ratios $\mu_1 = \mu_2 = 2$.

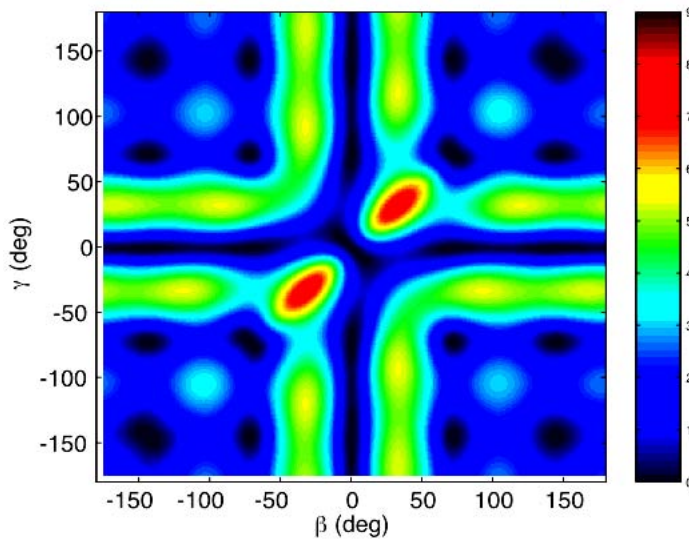


Figure 26. Relative array gain for an MVDR beam in 2D isotropic noise with discrete interferences at bearings β and γ , and interference-to-isotropic power ratios $\mu_1 = \mu_2 = 2$.

7. Discussion of results

This report defines the theoretical performance of conventional and adaptive beamformers for DIFAR-like sensors. A DIFAR-like sensor is defined as a sensor module containing either the first three or all five of the following elements: an omnidirectional element, two orthogonal horizontal dipole elements, and two horizontal quadrupole elements spaced 45 degrees in azimuth.

The performance measure for comparing sensors and beamforming methods is array gain. In this memorandum expressions were derived that allow array gain to be calculated directly from the cross spectral density matrix. For a three-element DIFAR-like sensor, the maximum array gain was found to be 6 dB in a 3D isotropic noise background and 4.77 dB in a 2D isotropic noise background. For a five-element DIFAR-like sensor, the maximum array gain was found to be 8.45 dB in a 3D isotropic noise background and 6.99 dB in a 2D isotropic noise background. These array gains do not take the self noise of the various sensing elements into account. If sensor self noise is comparable or higher than ambient noise the array gain will be degraded.

Expressions for array gain of both conventional and MVDR beamformers operating in a background consisting of isotropic noise (2D or 3D) as well as discrete-bearing interferences were derived, and a number of specific examples have been presented graphically. Some general observations can be made from the figures.

As an example, consider the case of the three-element sensor in 3D isotropic noise and one discrete interference. The array gain for this case is shown in Figures 3 and 4. Figure 3 demonstrates that a conventional beamformer steered to zero degrees shows a peak in the array gain at bearings near 110 degrees and -110 degrees. The reason for this behaviour is the existence of nulls in the beamformer response at these bearings. On the other hand the array gain of an MVDR beamformer exhibits a high array gain over a much larger range of bearings, since the MVDR algorithm adapts the beam response in order to minimize the average output power. The relative array gain in Figure 5 is the difference between the array gains in Figures 4 and 3. This figure shows that for certain relatively large ranges of the interference bearing, the MVDR beamformer has a larger array gain.

Similar conclusions may be drawn from Figures 6, 7, and 8, which deal with the five-element sensor module. In this case, however, it can be seen that the conventional beamformer has four nulls in its bearing response. These occur near -150, -70, 70, and 150 degrees.

The examples with two discrete-bearing interferences, in Figures 15 to 25, are more difficult to interpret. In these figures, the array gain is plotted as a function of the bearings of two interferences of equal power level ($\mu = 2$). Some observations may be helpful. Consider Figure 15. Values on the diagonals of the plot correspond to both interferences being at the same bearing angle. The array gains on the diagonal are therefore identical to the values in Figure 3 for $\mu = 4$ (the red curve). Comparison of

Figure 15 (conventional beamformer) with Figure 16 (MVDR) clearly shows that MVDR produces high array gains over a much larger range of interference bearings (note the relative size of the green, yellow, or red areas). This is even more evident when comparing Figures 20 and 21, which plot the array gains for the five-element sensor case.

In general, the array gain results indicate that in noise backgrounds consisting only of isotropic noise, the maximum gains can be obtained with conventional beamforming. However, in the presence of one or two strong interferences the MVDR beamformer can provide substantially higher array gains.

8. References

1. Urick, R. J., *Principles of Underwater Sound* for Engineers, 2nd ed. McGraw-Hill, New York, (1975).
2. Cox, Henry, *Resolving Power and Sensitivity to Mismatch of Optimum Array Processors*, J. Acoust. Soc. Amer., Vol. 54, No 3, (1973), 771-785.
3. Dudgeon, Dan E. and Mersereau, Russel M., *Multidimensional Digital Signal Processing*, Prentice Hall, Englewood Cliffs, New Jersey, (1984), 312-315.
4. Van Veen, B., *Minimum Variance Beamforming*, in *Adaptive Radar Detection and Estimation*, Haykin, S. and Steinhardt, A., editors, John Wiley & Sons, New York, (1992), 161-236.
5. Capon, J., *High Resolution Frequency-Wavenumber Spectrum Analysis*, Proc. IEEE, 57, no. 8, (Aug. 1969) 1408-18.
6. Burdick, William S., *Underwater Acoustic System Analysis*, Prentice Hall, Englewood Cliffs, New Jersey, Second Edition, (1991), 280-302.
7. Cox, Henry, *Line Array Performance When the Signal Coherence Is Spatially Dependent*, J. Acoust. Soc. Amer., Vol. 54, No 6, (1973), 1743-1746.

Annex A

A.1 Cross-spectral density matrix for an extended DIFAR sensor module in 3D isotropic noise

Here, all the cross-spectral terms for a five-element DIFAR-like sensor module are defined for 3D isotropic noise.

A.1.1 Cross-spectral terms for an extended DIFAR module

Each extended DIFAR sensor module has five co-located elements with directional responses (omni, y-axis dipole, x-axis dipole, quadrupole 1, and quadrupole 2) defined at a single location. Cross-spectral density can be summarized in a matrix as follows.

$$\mathbf{R} = \begin{bmatrix} Q(0,0) & Q(0,1) & Q(0,2) & Q(0,3) & Q(0,4) \\ Q(1,0) & Q(1,1) & Q(1,2) & Q(1,3) & Q(1,4) \\ Q(2,0) & Q(2,1) & Q(2,2) & Q(2,3) & Q(2,3) \\ Q(3,0) & Q(3,1) & Q(3,2) & Q(3,3) & Q(3,4) \\ Q(4,0) & Q(4,1) & Q(4,2) & Q(4,3) & Q(4,4) \end{bmatrix}. \quad (\text{A1})$$

The term $Q(m,n)$ in the above is evaluated from the following expression (Equation 29 in the text), repeated here for convenience as A2.

$$Q(m,n) = K \int_{-\pi}^{\pi} \int_{-\pi/2}^{\pi/2} D_m(\theta, \phi) D_n(\theta, \phi) \cos \phi d\phi d\theta, \quad (\text{A2})$$

where $D_m(\theta, \phi)$ and $D_n(\theta, \phi)$ denote the directional response of element- m and element- n respectively. The following results are obtained from Equation A2.

$$Q(0,0) = K \int_{-\pi}^{\pi} \int_{-\pi/2}^{\pi/2} \cos \phi d\phi d\theta = 4\pi K \quad (\text{A3})$$

$$Q(1,1) = K \int_{-\pi}^{\pi} \int_{-\pi/2}^{\pi/2} \cos^3 \phi \cos^2 \theta d\phi d\theta = \frac{4\pi K}{3} \quad (\text{A4})$$

$$Q(2,2) = K \int_{-\pi}^{\pi} \int_{-\pi/2}^{\pi/2} \cos^3 \phi \sin^2 \theta d\phi d\theta = \frac{4\pi K}{3} \quad (\text{A5})$$

$$Q(3,3) = K \int_{-\pi}^{\pi} \int_{-\pi/2}^{\pi/2} \cos^2 2\theta \cos^3 \phi d\phi d\theta = \frac{4\pi K}{3} \quad (\text{A6})$$

$$Q(4,4) = K \int_{-\pi}^{\pi} \int_{-\pi/2}^{\pi/2} \sin^2 2\theta \cos^3 \phi d\phi d\theta = \frac{4\pi K}{3} \quad (\text{A7})$$

The off-diagonal terms are zero for an isotropic noise background. For example,

$$Q(1,2) = K \int_{-\pi}^{\pi} \int_{-\pi/2}^{\pi/2} \cos^3 \phi \cos \theta \sin \theta d\phi d\theta = 0 \quad (\text{A8})$$

Annex B

B.1 Cross-spectral density matrix for an extended DIFAR sensor module in 2D isotropic noise

Here, all the cross-spectral terms for a five-element DIFAR-like sensor module are defined for 2D isotropic noise.

B.1.1 Cross-spectral terms for an extended DIFAR module

Each extended DIFAR sensor module has five co-located elements with directional responses (omni, y-axis dipole, x-axis dipole, quadrupole 1, and quadrupole 2) defined at a single location. Cross-spectral density can be summarized in a matrix as follows.

$$\mathbf{R} = \begin{bmatrix} Q(0,0) & Q(0,1) & Q(0,2) & Q(0,3) & Q(0,4) \\ Q(1,0) & Q(1,1) & Q(1,2) & Q(1,3) & Q(1,4) \\ Q(2,0) & Q(2,1) & Q(2,2) & Q(2,3) & Q(2,3) \\ Q(3,0) & Q(3,1) & Q(3,2) & Q(3,3) & Q(3,4) \\ Q(4,0) & Q(4,1) & Q(4,2) & Q(4,3) & Q(4,4) \end{bmatrix}. \quad (\text{B1})$$

Evaluation of the cross-spectral densities in 2D isotropic noise is most conveniently accomplished in the θ, ϕ (azimuth-elevation) coordinate system. A 2D isotropic noise model can be obtained from the 3D isotropic one by using a delta function $\delta(\phi - \xi)$ to create a noise model that is isotropic in azimuth, but has an impulse-like distribution $\delta(\phi - \xi)$ in elevation. The expression for cross-spectral density, from Equation 30, is given by

$$Q(m,n) = K \cos \xi \int_0^{2\pi} D_m(\theta, \xi) D_n(\theta, \xi) d\theta, \quad (\text{B 2})$$

where $D_m(\theta, \xi)$ and $D_n(\theta, \xi)$ denote the directional response of element- m and element- n respectively. The following results are obtained from Equation B2 with ξ set to zero, the value for horizontally propagating noise.

$$Q(0,0) = K \int_0^{2\pi} d\theta = 2\pi K \quad (\text{B 3})$$

$$Q(1,1) = K \int_0^{2\pi} \cos^2 \theta d\theta = \pi K \quad (\text{B } 4)$$

$$Q(2,2) = K \int_0^{2\pi} \sin^2 \theta d\theta = \pi K \quad (\text{B } 5)$$

$$Q(3,3) = K \int_0^{2\pi} \cos^2 2\theta d\theta = \pi K \quad (\text{B } 6)$$

$$Q(4,4) = K \int_0^{2\pi} \sin^2 2\theta d\theta = \pi K \quad (\text{B } 7)$$

The off-diagonal terms are zero for an isotropic noise background. For example,

$$Q(1,2) = K \int_0^{2\pi} \sin \theta \cos \theta d\theta = 0 \quad (\text{B } 8)$$

DOCUMENT CONTROL DATA

(Security classification of title, body of abstract and indexing annotation must be entered when the overall document is classified)

1. ORIGINATOR (the name and address of the organization preparing the document. Organizations for whom the document was prepared, e.g. Establishment sponsoring a contractor's report, or tasking agency, are entered in section 8.) Defence Research Establishment Atlantic 9 Grove Street, PO Box 1012 Dartmouth, NS B2Y 3Z7		2. SECURITY CLASSIFICATION (overall security classification of the document including special warning terms if applicable). <p align="center">UNCLASSIFIED</p>	
3. TITLE (the complete document title as indicated on the title page. Its classification should be indicated by the appropriate abbreviation (S,C,R or U) in parentheses after the title). <p align="center">Array gain of DIFAR-like Sensors</p>			
4. AUTHORS (Last name, first name, middle initial. If military, show rank, e.g. Doe, Maj. John E.) <p align="center">Maksym, Joseph N.</p>			
5. DATE OF PUBLICATION (month and year of publication of document) <p align="center">December 2001</p>		6a. NO. OF PAGES (total containing information Include Annexes, Appendices, etc). <p align="center">51</p>	6b. NO. OF REFS (total cited in document) <p align="center">7</p>
7. DESCRIPTIVE NOTES (the category of the document, e.g. technical report, technical note or memorandum. If appropriate, enter the type of report, e.g. interim, progress, summary, annual or final. Give the inclusive dates when a specific reporting period is covered). <p align="center">Technical Memorandum</p>			
8. SPONSORING ACTIVITY (the name of the department project office or laboratory sponsoring the research and development. Include address). Defence Research Establishment Atlantic PO Box 1012 Dartmouth, NS, Canada B2Y 3Z7			
9a. PROJECT OR GRANT NO. (if appropriate, the applicable research and development project or grant number under which the document was written. Please specify whether project or grant). <p align="center">Project 11cc</p>		9b. CONTRACT NO. (if appropriate, the applicable number under which the document was written).	
10a. ORIGINATOR'S DOCUMENT NUMBER (the official document number by which the document is identified by the originating activity. This number must be unique to this document.) <p align="center">DREA TM 2001-204</p>		10b. OTHER DOCUMENT NOS. (Any other numbers which may be assigned this document either by the originator or by the sponsor.)	
11. DOCUMENT AVAILABILITY (any limitations on further dissemination of the document, other than those imposed by security classification) (<input checked="" type="checkbox"/>) Unlimited distribution () Defence departments and defence contractors; further distribution only as approved () Defence departments and Canadian defence contractors; further distribution only as approved () Government departments and agencies; further distribution only as approved () Defence departments; further distribution only as approved () Other (please specify):			
12. DOCUMENT ANNOUNCEMENT (any limitation to the bibliographic announcement of this document. This will normally correspond to the Document Availability (11). However, where further distribution (beyond the audience specified in (11) is possible, a wider announcement audience may be selected).			

13. **ABSTRACT** (a brief and factual summary of the document. It may also appear elsewhere in the body of the document itself. It is highly desirable that the abstract of classified documents be unclassified. Each paragraph of the abstract shall begin with an indication of the security classification of the information in the paragraph (unless the document itself is unclassified) represented as (S), (C), (R), or (U). It is not necessary to include here abstracts in both official languages unless the text is bilingual).

This technical memorandum presents a theoretical comparison of array gains obtained with conventional and adaptive beamforming of DIFAR-like sensors. For the purposes of the memorandum, a DIFAR-like sensor is modeled by an omnidirectional element and two orthogonal horizontal dipole elements. Also considered, is an extended DIFAR-like sensor, in which the three-element sensor module is augmented by two horizontal quadrupole elements. A difficult problem in the design of beamformers is how to decide when to use an adaptive beamforming algorithm rather than a conventional beamformer. Basing the decision on data observed during sea trials can be misleading because the relative performance depends heavily on the acoustic environment. The problem can be simplified by comparisons of candidate beamforming techniques with a set of baseline acoustic noise backgrounds, namely 2D and 3D isotropic noise, with the addition of one or two discrete-bearing sources of interference. Mathematical expressions for array gain are derived, and graphical results are shown for the baseline acoustic noise backgrounds. It should be noted that the calculations in this memorandum have assumed that sensor self noise is negligible compared to background noise. This is not likely to be true in practice, especially with dipole and quadrupole sensing elements. To take self noise into account, one needs only to add the appropriate sensor self-noise powers to the diagonal of the cross spectral density matrix in the array gain expressions.

14. **KEYWORDS, DESCRIPTORS or IDENTIFIERS** (technically meaningful terms or short phrases that characterize a document and could be helpful in cataloguing the document. They should be selected so that no security classification is required. Identifiers, such as equipment model designation, trade name, military project code name, geographic location may also be included. If possible keywords should be selected from a published thesaurus. e.g. Thesaurus of Engineering and Scientific Terms (TEST) and that thesaurus-identified. If it not possible to select indexing terms which are Unclassified, the classification of each should be indicated as with the title).

Sonobuoys; DIFAR; Adaptive Beamforming; Array Gain; MVDR

This page intentionally left blank.

Defence R&D Canada

Canada's leader in defence
and national security R&D

R & D pour la défense Canada

Chef de file au Canada en R & D
pour la défense et la sécurité nationale



www.drdc-rddc.gc.ca